Pan *et al.*
Chinese Journal of Mechanical Engineering (2024) 37:80
https://doi.org/10.1186/s10033-024-01062-0

Chinese Journal of Mechanical Engineering

ORIGINAL ARTICLE

Open Access

Effect of Ellipsoidal Particle Shape on Tribological Properties of Lubricants Containing Nanoparticles

Ling Pan[1,2*], Zhi Li[1], Yunhui Chen[1] and Guobin Lin[2]

Abstract

Adding nanoparticles can significantly improve the tribological properties of lubricants. However, there is a lack of understanding regarding the influence of nanoparticle shape on lubrication performance. In this work, the influence of diamond nanoparticles (DNPs) on the tribological properties of lubricants is investigated through friction experiments. Additionally, the friction characteristics of lubricants regarding ellipsoidal particle shape are investigated using molecular dynamics (MD) simulations. The results show that DNPs can drastically lower the lubricant's friction coefficient μ from 0.21 to 0.117. The shearing process reveals that as the aspect ratio (a) of the nanoparticles approaches 1.0, the friction performance improves, and wear on the wall diminishes. At the same time, the shape of the nanoparticles tends to be spherical. When $0.85 \le a \le 1.0$, rolling is ellipsoidal particles' main form of motion, and the friction force changes according to a periodic sinusoidal law. In the range of $0.80 \le a < 0.85$, ellipsoidal particles primarily exhibit sliding as the dominant movement mode. As a decreases within this range, the friction force progressively increases. The friction coefficient μ calculated through MD simulation is 0.128, which is consistent with the experimental data.

Keywords Molecular dynamics simulation, Nanoparticle additives, Ellipsoidal particles, Tribological properties

1 Introduction

Lubricants are employed to lessen the friction and wear of machines. With the continuous advancement of science and technology, traditional lubricants have gradually become inadequate in meeting the evolving industry requirements for reduced friction and minimized wear volume. In that regard, lubricants containing nanoparticles have attracted significant attention from researchers due to their remarkable tribological properties, establishing themselves as increasingly vital materials in recent years. According to several studies, friction can be reduced by up to 80% using lubricants containing nanoparticles instead of basic lubricants [1, 2].

Nanoparticle additives improve the friction performance of lubricants mainly because of the rolling effect, tribofilm formation, mending, and polishing effects [3–5]. Numerous experiments have demonstrated the attractive tribological properties of nanoparticles as additives. For instance, Alias et al. [6] investigated the friction coefficient μ of lubricants with different contents of diamond nanoparticles (DNPs), concluding that the addition of DNPs reduced the value of μ from 0.40 to 0.12. Igarashi et al. [7] prepared phenol/formaldehyde resin-based composites with carbon nanotubes (CNTs) and found that CNTs effectively decreased the friction coefficient and wear of the phenolic resin. Yu et al. [8] have established that physically deposited graphite nanoparticles can form a film on the friction surface of vegetable oil, thereby improving anti-friction and

*Correspondence:
Ling Pan
panling@fzu.edu.cn
[1] School of Advanced Manufacturing, Fuzhou University, Quanzhou 362251, Fujian, China
[2] School of Mechanical Engineering and Automation, Fuzhou University, Fuzhou 350108, Fujian, China

anti-wear characteristics. Moreover, the friction coefficient and the degree of wear were shown to be related to the volume fraction and size of graphite nanoparticles.

However, analyzing nanoparticles' motion state and tribological properties in actual production is challenging because their size covers the micro-nano scale. In recent years, many researchers have used molecular dynamics (MD) simulations to quantitatively calculate tribological performance parameters that are difficult to measure in experiments [9–11]. Pan et al. [12, 13] applied the MD method to study the effects of carbon content and shear rate of naphthenic hydrocarbons on the boundary lubrication and interfacial slip. Gao et al. [14] employed a single-peak contact model, and Mo et al. [15] used a multi-peak contact model, pointing out that the friction force is proportional to the contact area. Han et al. [16] explored the tribological properties of Cu and Fe composite structures through the MD simulation. Zhang et al. [17] analyzed the nanoscale distribution characteristics of lubricant additives. Their findings revealed that surface adsorption was primarily influenced by molecular polarity, arrangement, and orientation. These factors are crucial for comprehending the mechanisms underlying nanoscale lubrication.

Most studies have primarily focused on examining the impact of nanoparticle properties on friction performance [18, 19]. However, the influence of particle shape on the anti-wear and anti-friction performance has remained largely unexplored. In earlier simulation studies, most nanoparticles were simplified as regular spheres, neglecting the potential impact of irregularly shaped nanoparticles on the lubricating system [20, 21]. However, the produced nanoparticles may have inconsistencies in aspect ratios (α) due to their small size.

Considering the research gaps mentioned above, this study aims to investigate, for the first time, the influence of DNPs on the tribological properties of base oil through friction experiments. MD simulation was used to explore the effect of nanoparticle aspect ratio α variation on lubricant lubrication performance. N-hexadecane was taken as the base oil to simulate nanoparticle additives' role in lubricating oil accurately. The diamond nanoparticle choice was due to their zero environmental impact and high hardness against the substrate. After altering the α of the nanoparticle and the external load, the motion state of the particles between the walls was analyzed. Subsequently, the impact of varying ellipsoidal particle aspect ratios on the tribological properties of the lubricant was examined by calculating the mechanical response and stress of the solid wall. This analysis shows how particle aspect ratio changes affect the lubricant's performance.

2 Experimental Details

The main instruments used in the experiment were the MFT-5000 tribo-wear tester (Figure 1) (Rtec Instruments Ltd.) and the Olympus LEXT OLS4100 3D measuring laser microscope. Given the low cost and convenience of extraction, DNPs acquired from Fuhua Mineral Materials were chosen as the nano-additive for the friction experiment. N-hexadecane (98% purity) purchased from McLean Reagent Network served as the base oil. A 20 × 20 × 10 mm Cu slab (Ra = 0.69 μm and the hardness is 170 HV) with a hardness much lower than that of diamond was used as the substrate and steel balls (E52100 and the hardness is 500 HV) with a diameter of 6.35 mm were selected as the indenter material (both were purchased from Zetian Metal Materials). Table 1 displays the key metrics for the friction experiment.

The ratio of the semi-major axis a and the semi-minor axis c of the ellipsoid is defined as the aspect ratio α of the diamond particle, which determines the nanoparticle shape (Figure 2).

Due to its low cost and high efficiency, the shock-wave method has been widely applied in industrial production to prepare nano-diamond particles [22]. Since the prepared diamond nanoparticles are easy to agglomerate, it is necessary to disperse them by mechanical or inorganic chemical methods [23]. After that, the nanoparticles were screened many times by

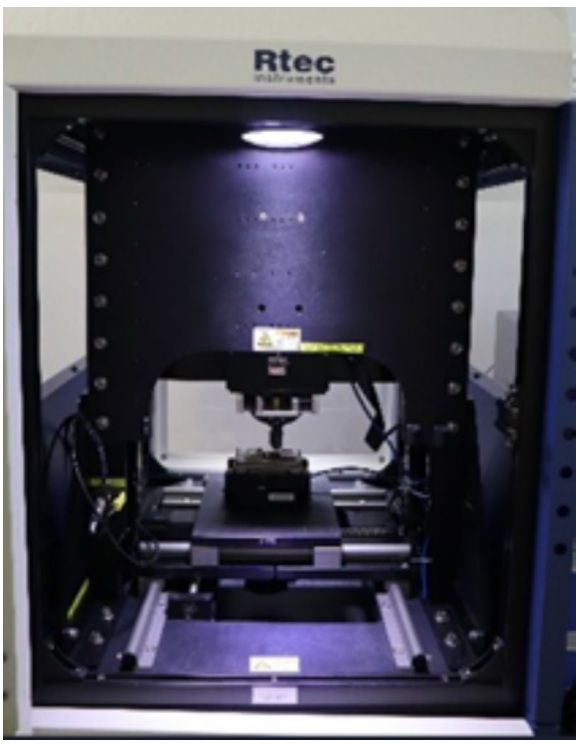

Figure 1 MFT-5000 friction and wear testing machine

Table 1 Parameters of the friction experiment

Metrics for experiment	
Motion mode	Reciprocating
Additives	DNPs
Temp	25 ℃
Load	1 N
Frequency	5 Hz
Time	30 min
Sliding stroke	5 mm

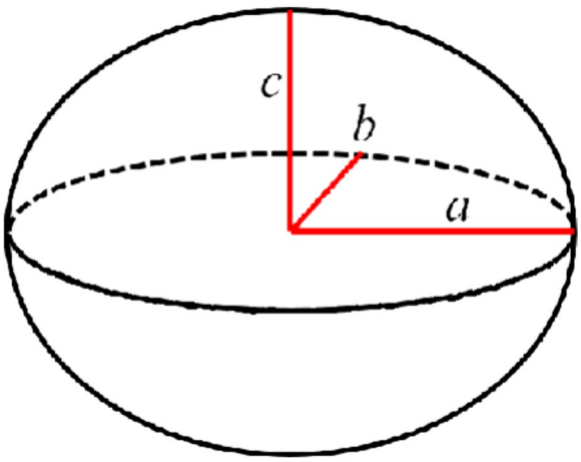

Figure 2 Ellipsoidal nanoparticle

membrane separation and other screening methods to obtain particles with different α [24]. The transmission electron microscopy (TEM) image of the DNPs used in the friction experiment is shown in Figure 3, where the primary range of α is between 0.88 and 0.98. This study aims to provide a theoretical foundation for producing nano-diamond particles.

The results of the friction experiment are shown in Figure 4. The friction coefficient μ of pure n-hexadecane gradually increases and remains stable at about 0.21 after 1000 s. After adding DNPs, the value of μ is still lower than that of pure base oil, at 0.117 ± 0.003 after 1000 s. Figure 5 displays the wear scar morphology of the sample under a three-dimensional measuring laser microscope. It can be found that the addition of nano-additives reduces the wear scar width from 0.51 mm to 0.43 mm.

Figure 6 is the SEM image of wear scar morphology. Figures 6a and b show the wear pattern under 100-fold electron microscope. When the lubricant is pure n-hexadecane, and nano-diamond is added, wear marks are deeper and more noticeable. The wear patterns under 500-fold electron microscopy are displayed in Figure 6c and d. Traces of adhesive wear are seen in Figure 6c and are indicated in red circles. Lubricants containing nano-diamonds reduce the wear significantly.

3 Molecular Dynamics Simulations

3.1 Establishment of the Molecular Dynamics Model

Figure 7 depicts a boundary lubrication model containing nano-ellipsoid particles. The upper and lower walls are made of face-centered cubic (FCC) crystalline copper, and the wall thickness is 2.8 nm. The dimensions of the boundary lubrication model in the x and y directions are 14.3 nm × 7.2 nm. The periodic boundary conditions are applied in the x and y directions, and the aperiodic boundary conditions are valid in the z direction. The upper and lower solid walls were divided into three layers for the analysis. These layers consist of an inner Newtonian layer that reflects the mechanical response, an intermediate thermostat layer that regulates the system's temperature, and a rigid layer that enforces the boundary conditions. This division ensures a more comprehensive understanding of the system's behavior and enables accurate characterization of the tribological properties. Only a limited number of *n*-hexadecane molecules is positioned between the upper and lower walls in the boundary lubrication because most base oil molecules will be pushed out of the contact area of the rough body [25]. Diamond nanoparticles (DNPs) are utilized as an additive and assumed to be the rigid bodies in the simulation to prevent their deformation during the motion and avoid a negative impact on the data accuracy. The parameter α of the nanoparticles used in the MD simulation is shown in Table 2.

3.2 Details of the Simulation

The united-atom force fields model (TraPPE-UA) [26] can be employed to simulate the interactions between hexadecane molecules. This model simplifies the internal forces within the molecules by utilizing pseudo-atoms that represent the CHx groups. These pseudo-atoms are positioned at the carbon atom's locations, reducing computational complexity while maintaining the required accuracy. The necessary calculations can be performed efficiently without compromising the reliability of the simulation results by employing the TraPPE-UA model. The interactions between Cu atoms are described by the EAM potential function [27] to reflect the deformation of the wall. The interactions between C and Cu atoms adopt the Morse potential [20, 28], providing faster calculation speed and higher precision. In the simulation, diamond nanoparticles are regarded as rigid bodies, and the forces between their internal atoms are ignored [29]. The non-bonding interactions between other atoms can be reproduced using the L-J potential [30].

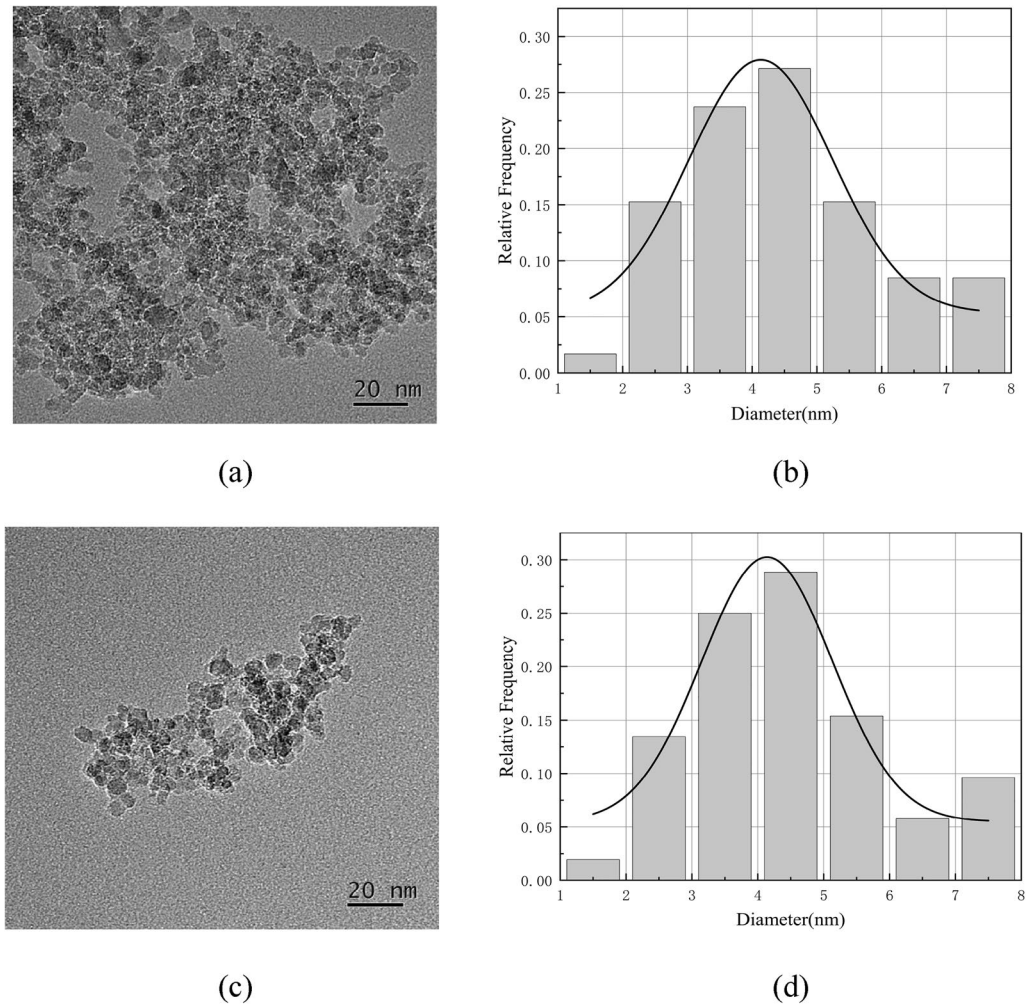

Figure 3 TEM image of DNPs: **a**, **c** TEM image of DNPs, **b**, **d** Respective diameter distributions of DNPs

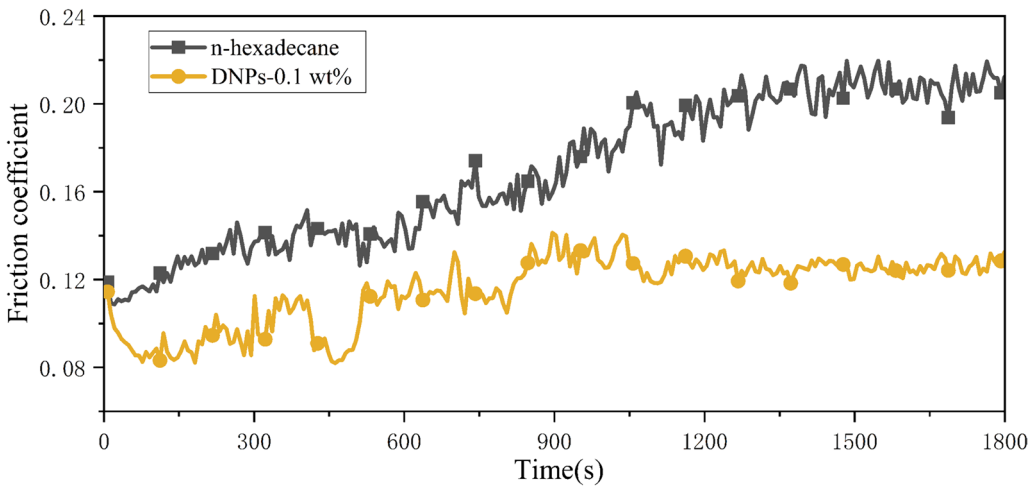

Figure 4 Friction coefficients of different lubricants under 1 N load as a function of time

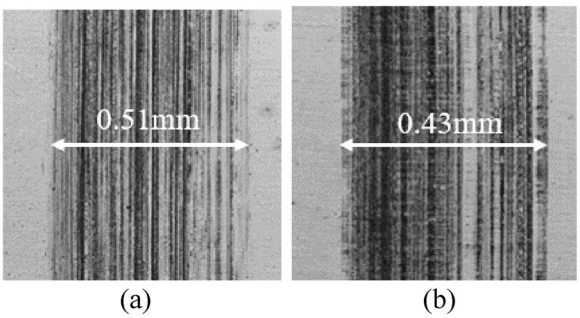

Figure 5 The abrasion marks under a three-dimensional measuring laser microscope: **a** N-hexadecane, **b** DNPs-0.1 wt%

The friction and wear process of the entire boundary lubrication system includes three stages: relaxation, compression, and shear. The system's energy is first minimized, followed by relaxation under the NVT ensemble, so the system's energy converges to a constant value. Subsequently, the system transitions into the dynamic compression stage, where the NVE ensemble is employed instead of the NVT ensemble. The effect of compression is achieved by fixing the rigid layer 2 and exposing the rigid layer 1 to an external load. At the beginning of the pressurization stage, a pressure of 30 MPa is first applied to the rigid layer 1 along the z direction to ensure the stability of the model. After the system height is gradually stabilized, the pressure is

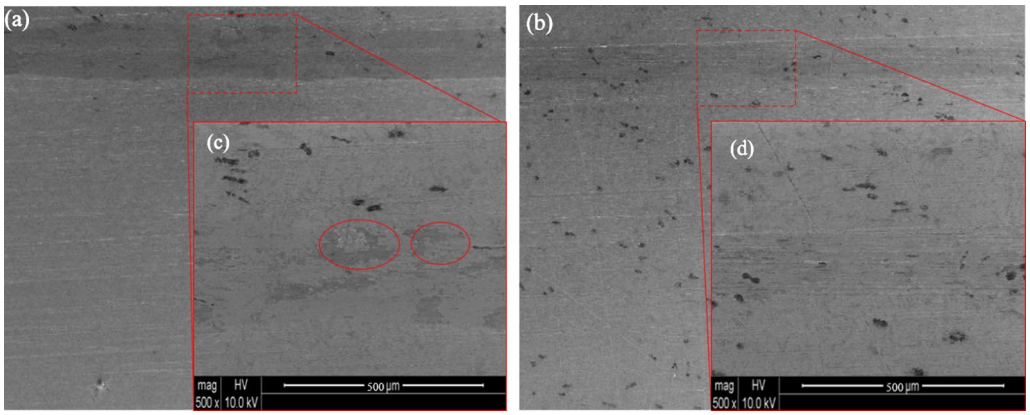

Figure 6 SEM image of wear scar morphology: **a** 100X-N-hexadecane,**b** 100X-DNPs-0.1 wt%, **c** 500X-N-hexadecane, **d** 500X-DNPs-0.1 wt%

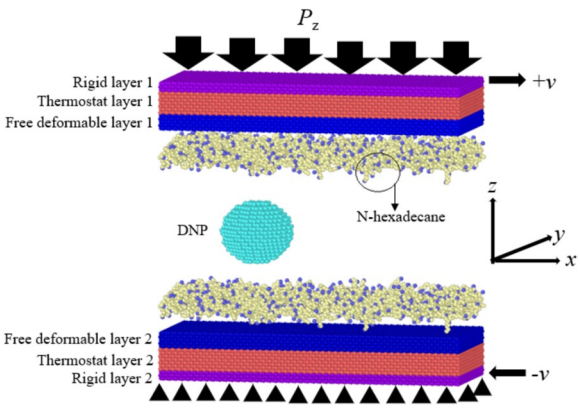

Figure 7 Boundary nano-lubricant model

Table 2 Parameters of ellipsoidal particles

$a = c/a$	0.80	0.83	0.85	0.88	0.9	0.95	1.0
$a = b$ (nm)	2.30						
c (nm)	1.85	1.91	1.96	2.03	2.07	2.19	2.30

further increased from 300 to 600 MPa. Because of the presence of nanoparticles and base oil molecules, there is no direct contact between the upper and lower walls. The Nose-Hoover method [31] controls the temperature of layers 1 and 2 at a constant value of 300 K to conduct the heat generated by the system. During the shearing phase at a constant pressure, the oppositely oriented velocities v with equal magnitudes are applied in the x-direction of rigid layers 1 and 2. The pressing time is 0.2 ns, and the shearing time is 1.8 ns. In the entire molecular dynamics (MD) simulation, a time step of 1 fs is used. The damping coefficient is also set to 100 times the time step size.

4 Results and Discussion

4.1 Shear Stage

The positive direction of particle rolling was clockwise to distinguish it from the other possible directions. Figure 8 depicts the front views of various lubrication systems at different times when the pressure (P_z) is 300 MPa, and the speed (v) is 10 m/s. It can be found that most of the base oil molecules are closely distributed near the wall, forming an adsorption layer. During t = 0.25-0.40 ns, nanoparticles will roll in all cases, and their rolling speed increases rapidly with the aspect ratio α. After that, the shearing action causes the particles with smaller α (α < 0.85) to slide relative to the walls rather than roll.

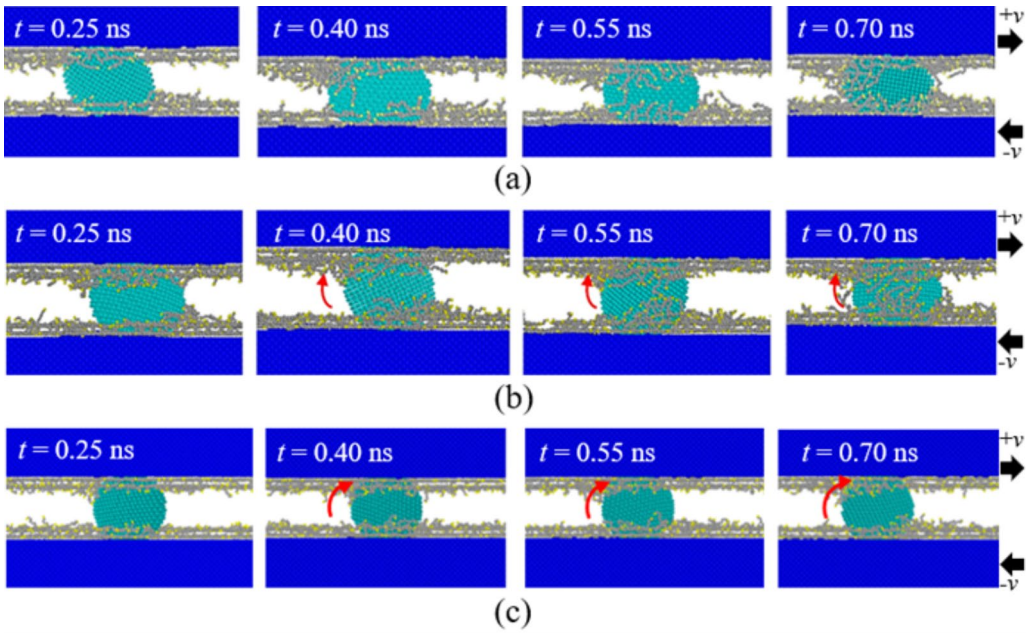

Figure 8 Front views of the lubrication system at different moments: **a** α = 0.83, **b** α = 0.88, **c** α = 1.0

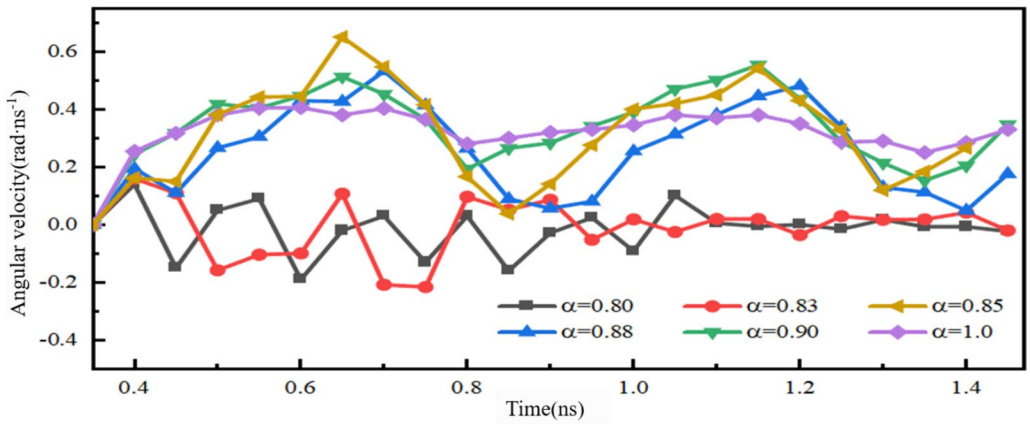

Figure 9 Particle angular velocity ω as a function of time under P_z = 300 MPa

Particles with larger values of α ($0.85 \leq \alpha \leq 1.0$) will predominantly exhibit a rolling motion. This motion is primarily because particles with shapes closer to a sphere experience reduced rolling resistance against the upper and lower walls.

Figure 9 displays the particle angular velocity ω as a function of time t at P_z = 300 MPa, which further reflects the motion state of particles with different values of α during the shearing process. During the initial shearing stage (t < 0.40 ns), particles with various α values all exhibit a clockwise rolling motion in tandem with the shearing movement. Furthermore, the angular velocity of the particles increases with higher α values. At t = 0.40-0.45 ns, the angular velocity of the particles with α < 0.85 turns from positive to negative and then oscillates between -0.2 and 0.2 rad/ns, which is because the particles sway from side to side due to the action of the wall. At t > 1.05 ns, the fluctuation amplitude of the particle angular velocity at α < 0.85 tends to zero, indicating that the particle is sliding in the subsequent motion process. The positive particle exhibits sinusoidal variation at $0.85 \leq \alpha < 1.0$ during the entire shearing process. In addition, the larger the value α of the particles, the higher the average of ω and the smaller the fluctuation amplitude, meaning that the particle has a quasi-spherical shape and the rolling is more likely to occur. When α = 1.0, the particle is spherical, and its angular velocity gradually stabilizes around 0.3 rad/ns after t = 0.6 ns.

To analyze the wear abrasion of the walls with different values α in a lubrication system, the surface topography maps of the lower wall were acquired at P_z = 300 MPa and t = 0.65 ns (see Figure 10). From blue to red, the height of Cu atoms along the z-direction changes from negative to positive. This also means that red indicates the higher height of the surface atoms, while dark blue denotes the appearance of grooves on the surface. According to Figure 10a, it can be seen that grooves with different depths are on the wall under the sliding action of nanoparticles with α = 0.80. Moreover, the lattice distortion of Cu atoms occurs under the extrusion action along the two sides of the groove. Besides, the atoms accumulate in front of the movement of nanoparticles. In Figure 10b, the nanoparticles with α = 0.83 also exhibit sliding motion. However, the wear on the wall surface is noticeably less severe compared to the lubrication system with α = 0.80. In Figure 10c, the nanoparticles continue to roll throughout the shearing process, and no grooves, atomic stacking, or ridges are observed on the wall's surface. However, some wall atoms are found to be randomly distributed in the wear zones due to the stress concentration that occurs when the long-axis end of the particle is in contact with the wall, forming defects on the wall atoms [32].

The wear behavior of the lubricating system can be further revealed by calculating the number of atoms removed from the solid wall. If the displacement of a Cu atom is greater than half of the Cu lattice constant (0.18 nm), the atom is considered to be removed. Figure 11 depicts the number of wear atoms in the shearing process for the lubrication systems with α = 0.80 (sliding particles) and α = 0.90 (rolling particles) at P_z = 300 MPa and v = 10 m/s. It can be observed that the former removes more atoms than the latter throughout the shearing time. After t = 1.0 ns, the difference in the wear amount between the two systems becomes larger. With the increase of time, the wear amount of the sliding particles continues to increase. In contrast, that of the

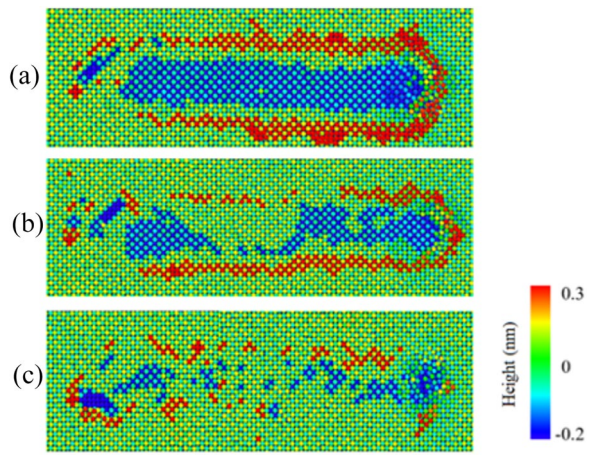

Figure 10 Variation of atomic height on the lower wall along the z direction (P_z = 300 MPa and t = 0.65 ns): **a** α = 0.80, **b** α = 0.83, **c** α = 0.90

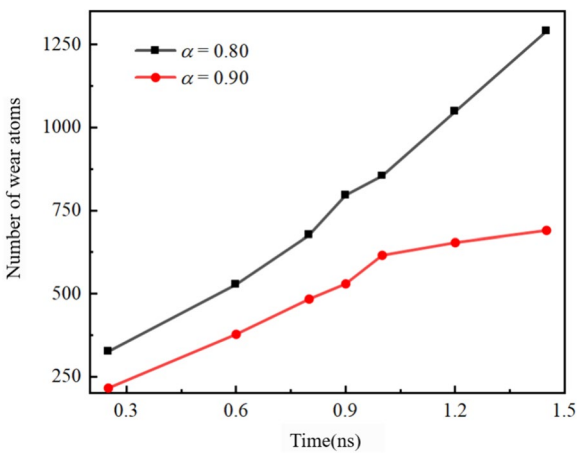

Figure 11 The atomic wear of the lubricating system in the shear process

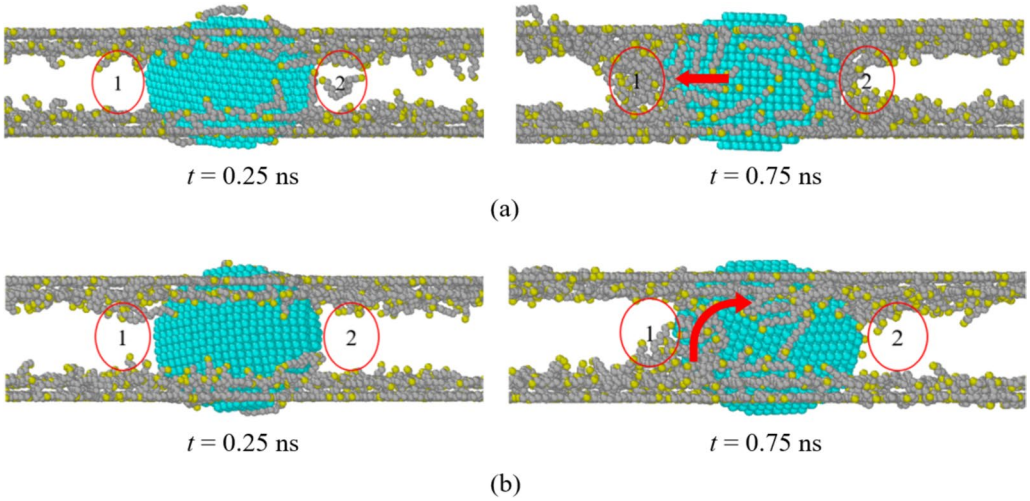

Figure 12 Front view without the wall lubrication system at P_z = 300 MPa and v = 40 m/s: **a** α = 0.80, **b** α = 0.90

rolling particles gradually decreases, proving that the wear induced by rolling nanoparticles is weaker than that caused by sliding nanoparticles.

Figure 12 depicts the front view of the lubricating oil film containing nanoparticles at different moments at P_z = 300 MPa and v = 20 m/s. It can be found that once the pressure is stabilized (t = 0.25 ns), the nanoparticles directly contact the solid wall, resulting in the deformation of the wall in the contact area. Under the influence of the particles, the lubricating oil molecules that have initially been adsorbed on the wall separate from its surface, then squeeze out of the contact zone and move around the particles. However, the direction of motion of oil molecules cannot form a complete closed loop. When t = 0.75 ns (Figure 12a), some base oil molecules are squeezed and aggregated around the particles. The number of molecules in region 1, the direction of particle sliding (shown with the red arrow in the figure), is significantly larger than in region 2. This phenomenon is also observed in Figure 12b. However, because of the rolling motion of nanoparticles, there is only a small amount of base oil molecular aggregates in the surrounding region 1, and the quantity of molecules in the region 2 remains almost unchanged. This observation means that the movement of particles will affect the adsorption behavior of base oil molecules on the wall during the shearing process. Sliding particles are more likely to cause molecular aggregation than rolling particles.

4.2 Mechanical Response

Figure 13 depicts the relationship between the friction force F_L of the lubricating system with different aspect ratios α and the time t at P_z = 300 MPa. For the convenience of observation, only one point is marked for every 10 data. In the lubricating system with α = 1.0 (spherical particles), the value of F_L is always stable (around 3.16 eV·Å^{-1}) during the shearing process. Furthermore, the nanoparticles primarily undergo rolling motion in this system. When 0.85 ≤ α < 1.0, the particles are kept rolling, and the F_L value of the system varies according to a sinusoidal law. With the decrease of α, the oscillation amplitude and the maximum of F_L of the system increase. When α < 0.85, the motion of nanoparticles is not just like the rolling during the shearing process, but a combination of rolling and sliding (rolling first and then sliding). Simultaneously, F_L is maintained high, with no obvious periodic variation.

In Figure 13a, the F_L value decreases from 6.28 eV·Å^{-1} to 0.02 eV·Å^{-1} in the lubricating system with α=0.90 within the time range of t = 0.55 - 0.69 ns. The nanoparticles rotate clockwise when they transition from the long-axis end to the short-axis end and engage in a rolling motion. As a result, the center of gravity gradually shifts downward, leading to a force between the nanoparticles and the wall that is opposite in direction to F_L. At 0.70 - 0.87 ns, the value of F_L increases from 1.08 eV·Å^{-1} to 9.20 eV·Å^{-1}, which is because the system needs to overcome the force between the wall and the particles to make the latter ones "stand up", thereby augmenting F_L. At t = 0.25-1.80 ns, the F_L parameter of the lubricating system with 0.85 ≤ α ≤ 1.0 varies as a sinusoidal function.

When α = 0.83 (Figure 13b), the lubricating system oscillates up and down at 8.78 eV·Å^{-1} at t = 0.40-0.70 ns. The interaction between nanoparticles and the wall during the shearing process tends to roll. However, since α is small, the long axis prevents it from rolling further.

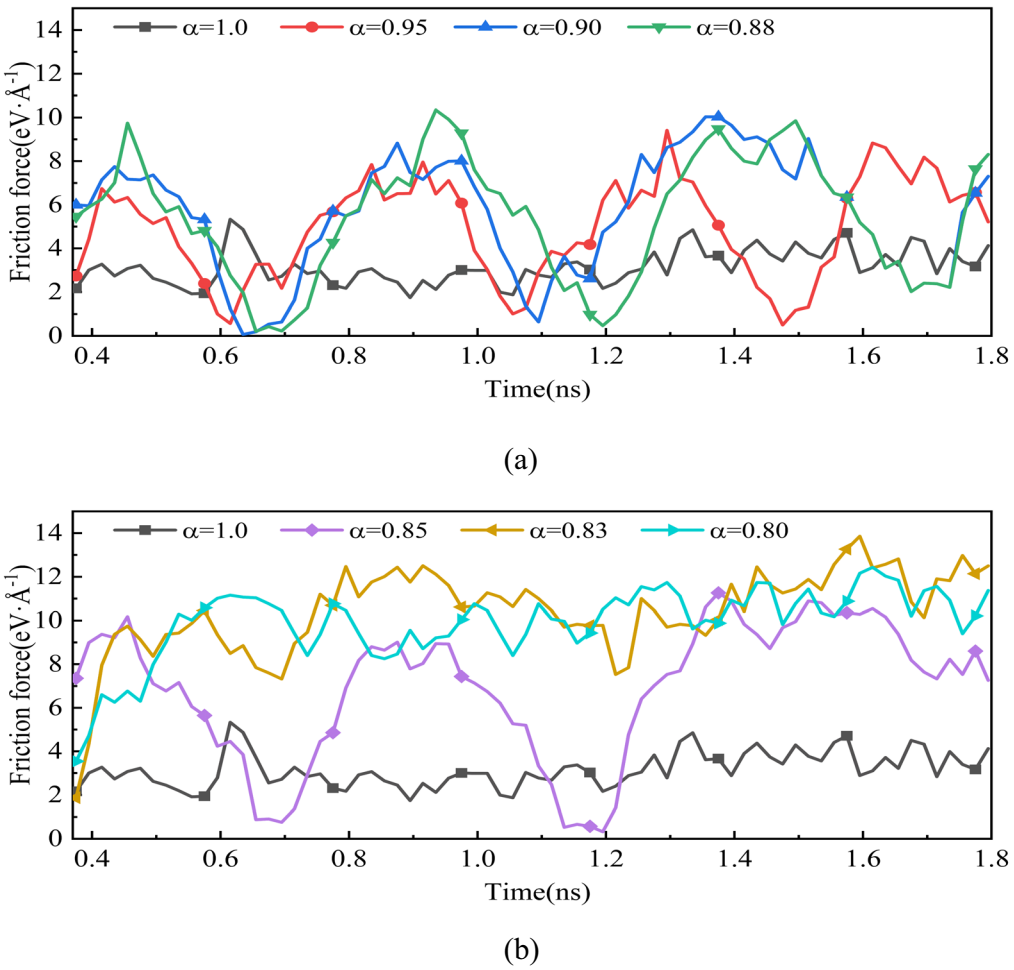

Figure 13 The values of F_L of the lubrication system with different particles at P_z = 300 MPa (1 point is marked at the interval between each 10 points): **a** 0.85 < $\alpha \leq$ 1.0, **b** $\alpha \leq$ 0.85

Then, the value of F_L increases to 11.13 eV·Å^{-1} due to the direct contact between the wall and the particle. This is because the lattice distortion of the Cu atoms in the contact area under the extrusion action hinders the movement of the wall, causing the F_L to increase. Compared to the lubrication system with $\alpha = 0.90$, the system with $\alpha = 0.83$ exhibits a 26.71% increase in the maximum friction force F_L. This suggests that rolling particles contribute to a lower peak in F_L. In addition, the F_L variation curve of the lubricating system with $\alpha = 0.80$ is similar to that of the system with $\alpha = 0.83$.

Nevertheless, the maximum F_L value of the former system is smaller than that of the latter. The nanoparticles in the former system are kept sliding, resulting in the relatively small fluctuation range of F_L. This may be due to the reduction in α, the flattened particle shape, and the enlarged contact area with the wall, reducing the stress concentration on the wall.

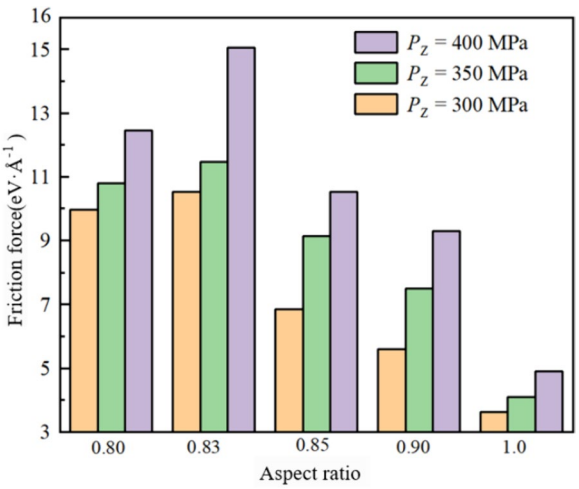

Figure 14 Friction force F_L of lubrication systems with different particle aspect ratios under different loads

Figure 14 depicts the friction force F_L of the particle lubricating system with different aspect ratios under various loads, which is the average over the whole shearing process. It can be found that when $\alpha = 1.0$, the rolling state of the particles can always be maintained so that F_L of the system achieves its minimum. In the case of $0.85 \leq \alpha < 1.0$, there is a slight increase in the F_L value of the system compared with spherical particles under three loading conditions, but it is still kept at a low level. At this time, the particles are mainly rolling during shearing, which also ensures good friction performance, and with the increase of α, the F_L of the system is further reduced. When $0.80 \leq \alpha < 0.85$, the particles are too flat to roll and slide between the two walls. At this time, the F_L value of the system decreases with the decrease of α, which is also consistent with the result observed in Figure 13.

At the micro-nano scale, the interactions between *n*-hexadecane molecules, wall atoms, and ellipsoid particle atoms are crucial in determining the tribological properties of the lubrication system. In this context, the conventional macroscopic friction force formula ($F_L = \mu \cdot F_N$) is no longer directly applicable due to the complex and intricate nature of these interactions. In this respect, Derjaguin [33] considered the role of adhesion and introduced a quantitative force L_0:

$$F_L = \mu(L_0 + F_N) = F_0 + \mu \cdot F_N, \quad (1)$$

where F_0 is the frictional force offset, F_N is the positive pressure, and μ is the friction coefficient.

The results obtained from the MD simulation were thus fitted using Eq. (1), and the friction coefficients μ of the lubricating systems with different α particles were obtained. As shown in Figure 15, the intercept of the fitted line is the frictional force offset, and the slope is the frictional factor. The friction force deviation of the lubricating system with $\alpha = 1.0$ is found to be -0.78 eV·Å^{-1}, and the μ value is 0.128, which is in line with that (0.12) determined in Ref. [6] and the above-measured value (0.117 ± 0.003). The frictional offset of the lubricating system with $\alpha = 0.90$ is -1.24 eV·Å^{-1}, and the value of μ is 0.169, 32% higher than that of particles with $\alpha = 1.0$. The frictional offset of the lubricating system with $\alpha = 0.80$ is 0.42 eV·Å^{-1}, and the value of μ is 0.251, i.e., 96% and 48% greater than those of particles with $\alpha = 1.0$ and $\alpha = 0.90$, respectively.

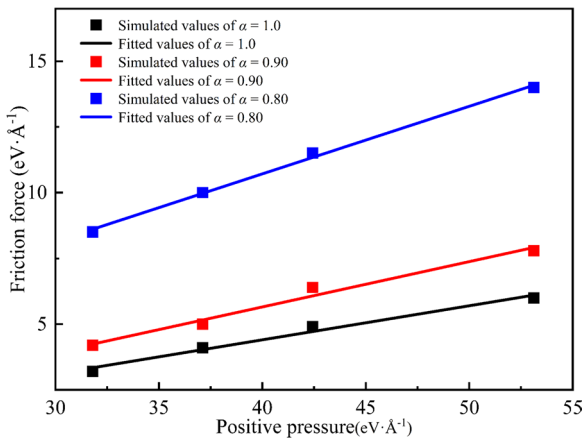

Figure 15 Friction coefficient μ of particle lubrication systems with different aspect ratios

5 Conclusions

The effects of nanoparticles as additives on lubricating systems under different loads and shear rates were analyzed experimentally and via MD simulations. The friction force and positive pressure obtained by the system were calculated by changing the shape of the nanoparticles, and the wear regularities of the walls were also observed. Based on the findings of this work, the following conclusions can be drawn.

(1) The experimental results of friction and wear show that adding DNPs with an aspect ratio of 0.88-0.98 can effectively improve the friction performance of n-hexadecane, reducing the average value of the friction coefficient μ by approximately 44.3%.
(2) During the shearing process, the motion of quasi-spherical nanoparticles at $0.85 \leq \alpha \leq 1.0$ is dominated by rolling. When $0.80 \leq \alpha < 0.85$, sliding is predominant. Moreover, the closer the nanoparticle shape to spherical (i.e., the nearer is α to 1.0 in the rolling movement), the smaller the friction coefficient of the lubricating oil and the weaker the wear undergone by the wall.
(3) When $0.85 \leq \alpha \leq 1.0$, the angular velocity of the rolling particle changes periodically according to a sinusoidal law. As the value of α increases, the fluctuation amplitude of the angular velocity rises, whereas that of the frictional force decreases. If $0.80 \leq \alpha < 0.85$, the angular velocity of the rolling particles gradually tends to 0, which means the sliding motion. Once the α parameter decreases, the contact area between the particles and the wall increases, and the friction force decreases instead.
(4) In the friction experiment, the addition of DNPs to the lubricant lowers the friction coefficient μ from 0.21 to 0.117 ± 0.003, and the results are consistent with that of the MD simulation of the particles (0.128).

The objective of this study is to establish a theoretical basis for the production of nano-diamond particles. On the basis of MD simulation, we hope to introduce

water molecules and oxygen atoms to simulate the friction behavior under real conditions. This will enable us to investigate friction phenomena more accurately at the molecular scale.

Supplementary Information

The online version contains supplementary material available at https://doi.org/10.1186/s10033-024-01062-0.

Supplementary material 1.

Supplementary material 2.

Acknowledgements
We are grateful to the Fujian Super Computing Center for providing computing support.

Author Contributions
LP was in charge of the whole trial; ZL wrote the manuscript; YC assisted with collating data; GL assisted with data visualization. All authors read and approved the final manuscript.

Funding
Supported by National Natural Science Foundation of China (Grant No. 52275178) and Fujian industry university cooperation project (Grant No. 2020H6025).

Data availability
Data will be made available on request.

Declarations

Competing Interests
The authors declare that they have no competing interests.

Received: 22 March 2023 Revised: 19 June 2024 Accepted: 27 June 2024
Published online: 29 July 2024

References

[1] M J G Guimarey, J M L del Rio, J Fernández. Improvement of the lubrication performance of an ester base oil with coated ferrite nanoadditives for different material pairs. *Journal of Molecular Liquids,* 2022, 350: 18550.
[2] V S Mello, E A Faria, S M Alves, et al. Enhancing Cuo nanolubricant performance using dispersing agents. *Tribology International,* 2020, 150: 106338.
[3] S Rahman, D Purani, S Ali, et al. Effects of SiO2 Contaminant on Thermo-Mechanical/Chemical Properties and Lubricity of PFPE Lubricants. *Lubricants,* 2021, 9 (9): 90.
[4] L L Bao, C Y Zhong, P F Jie, et al. The effect of nanoparticle size and nanoparticle aggregation on the flow characteristics of nanofluids by molecular dynamics simulation. *Advances in Mechanical Engineering,* 2019, 11 (11): 1687814019889486.
[5] Z Xuan, L H Su, G Y Deng, et al. Study on lubrication characteristics of C4-Alkane and nanoparticle during boundary friction by molecular dynamics simulation. *Metals,* 2021, 11(9): 1464.
[6] A A Alias, H Kinoshita, M Fujii. Tribological properties of diamond nanoparticle additive in water under a lubrication between steel plate and tungsten carbide ball. *Journal of Advanced Mechanical Design, Systems, and Manufacturing,* 2015, 9 (1): JAMDSM0006-JAMDSM0006.
[7] A Igarashi, T Terasawa, M Kanie, et al. A morphological study of the effect of carbon nanotube filler on tribology of phenol/formaldehyde resin-based composites. *Polymer Journal,* 2005, 37(7): 522-528.
[8] Y Su, L Gong, D Chen. An investigation on tribological properties and lubrication mechanism of graphite nanoparticles as vegetable based oil additive. *Journal of Nanomaterials,* 2015(1): 276753.
[9] R T Tong, G Liu, T X Liu. A local region molecular dynamics simulation method for nanoscale sliding contacts. *Chinese Journal of Mechanical Engineering,* 2018, 31: 18.
[10] T D Ta, H D Ta, K A Tieu, et al. Impact of chosen force fields and applied load on thin film lubrication. *Friction,* 2021, 9(5): 1259- 1274.
[11] A Takari, A R Ghasemi, M Hamadanian, et al. Molecular dynamics simulation and thermo-mechanical characterization for optimization of three-phase epoxy/TiO_2/SiO_2 nano-composites. *Polymer Testing,* 2021, 93: 106890.
[12] L Pan, S P Lu, H Yu, et al. Molecular dynamics simulates the effect of naphthenic carbon content on boundary lubrication. *Journal of Mechanical Engineering,* 2020, 56 (1): 110-118. (in Chinese)
[13] L Pan, X Q Xie, J Y Guo. Synergistic lubrication effects and tribological properties of graphene/oil-based lubricant systems. *Surface Topography: Metrology and Properties,* 2022, 51(11): 395- 404.
[14] G T Gao, R J Cannara, R W Carpick. Atomic-scale friction on diamond: a comparison of different sliding directions on (001) and (111) surfaces using MD and AFM. *Langmuir: the ACS Journal of Surfaces and Colloids,* 2007, 23(10): 5394-5405.
[15] Y F Mo, K T Turner, I Szlufarska. Friction laws at the nanoscale. *Nature,* 2009, 457(7233): 1116-1119.
[16] Y Q Han, L Pan, H Zhang, et al. Effect of lubricant additives of Cu, Fe and bimetallic CuFe nanoparticles on tribological properties. *Wear,* 2022, 508: 204485.
[17] G H Zhang, Y J Qiao, Y H Liu, et al. Molecular behaviors in thin film lubrication—Part one: Film formation for different polarities of molecules. *Friction,* 2019, 7(4): 372-387.
[18] S P Ju, I J Lee, H Y Chen. Melting mechanism of Pt–Pd–Rh–Co high entropy alloy nanoparticle: An insight from molecular dynamics simulation. *Journal of Alloys and Compounds,* 2021, 858: 157681.
[19] A Tomala, B Vengudusamy, M R Ripoll, et al. Interaction between selected MoS_2 nanoparticles and ZDDP tribofilms. *Tribology Letters,* 2015, 59 (1): 1-18.
[20] X Zhang, Z J Wang, H M Shen, et al. An efficient model for the frictional contact between two multiferroic bodies. *International Journal of Solids and Structures,* 2018, 130: 133-152.
[21] P E James, G Chiara, M T Foram, et al. Nonequilibrium molecular dynamics investigation of the reduction in friction and wear by carbon nanoparticles between iron surfaces. *Tribology Letters,* 2016, 63(3): 1-15.
[22] V N Mochalin, O Shenderova, D Ho, et al. The properties and applications of nano-diamonds. *Nature Nanotechnology*, 2012, 7(1): 11-23.
[23] X Zhao, Y L Liao, Y J Huang, et al. Research progress on dispersion method for nano-diamond. *Powder Metallurgy Technology*, 2021,39 (1): 15-23. (in Chinese)
[24] J C Liang, Z G Wang, M H Huang, et al. Effects on carbon molecular sieve membrane properties for a precursor polyimide with simultaneous flatness and contortion in the repeat unit. *ChemSusChem*, 2020, 13(20):5531-5538.
[25] J Q Shi, J Chen, L Fang, et al. Atomistic scale nanoscratching behavior of monocrystalline Cu influenced by water film in CMP process. *Applied Surface Science,* 2018, 435: 983- 992.
[26] M G Marcus, J I Siepmann. Transferable potentials for phase equilibria. 1. united-atom description of n-Alkanes. *The Journal of Physical Chemistry, B. Condensed Matter, Materials, Surfaces, Interfaces & Biophysical,* 1998, 102(14): 2569-2577.
[27] Y Mishin, M J Mehl, D A Papaconstantopoulos, et al. Structural stability and lattice defects in copper: Ab initio, tight-binding, and embedded-atom calculations. *Physical Review B,* 2001, 63(22): 77-81.
[28] P M Morse. Diatomic molecules according to the wave mechanics. II. vibrational levels. *Physical Review,* 1929, 34(1): 57-64.
[29] J Q Shi, L Fang, K Sun, et al. Surface removal of a copper thin film in an ultrathin water environment by a molecular dynamics study. *Friction,* 2019, 8(2): 323-334.
[30] J G Lee. *Computational materials science: An introduction.* 2nd ed. CRC Press, 2016.
[31] S Nose. An extension of the canonical ensemble molecular dynamics method. *Molecular Physics,* 1986, 57(1): 187-191.

[32] L Fang, K Sun, J Q Shi, et al. Movement patterns of ellipsoidal particles with different axial ratios in three-body abrasion of monocrystalline copper: a large scale molecular dynamics study. *RSC Advances,* 2017, 7 (43): 26790-26800.
[33] S J Eder, A Vernes, G Betz. On the Derjaguin offset in boundary-lubricated nanotribological systems. *Langmuir,* 2013, 29(45): 13760-13772.

Ling Pan received her Ph.D. degree from *Fuzhou University, China*, in 2015. She is presently a professor and master supervisor of *the School of Mechanical Engineering and Automation, Fuzhou University, China*. A senior member of the Chinese Mechanical Engineering Society and the director of the Fuzhou Friction and Lubrication Industry Technology Innovation Center. Her main research interests are tribology and mechanical design/theory.

Zhi Li a postgraduate student in *the School of Advanced Manufacturing at Fuzhou University*. He obtained a bachelor's degree from *Qingdao University* in 2020. His current research interest is tribology.

Yunhui Chen a postgraduate student in *the School of Advanced Manufacturing at Fuzhou University*. He obtained a bachelor's degree from *East China Jiaotong University* in 2021. His current research interest is tribology.

Guobin Lin received a master's degree from *Fuzhou University* in 2022. His main research interest is tribology.